NPL Report MOM 126 398

April 1995

A Novel 3-axis CMM Probe Calibration Facility

Richard K Leach
Division of Mechanical and Optical Metrology
National Physical Laboratory
Teddington
Middlesex
United Kingdom
TW11 OLW

ABSTRACT

A facility has been developed to calibrate co-ordinate measuring machine analogue probes to an accuracy of 0.1 µm. A high precision three-axis translation stage moves the probe stylus and the position of the stage is determined by three mutually-orthogonal laser interferometer transducers. The co-ordinates indicated by the probe are compared with the co-ordinates indicated by the interferometers and the errors of the probe are then calculated. The working volume of the facility is 2 x 2 x 2 mm. The full measurement strategy and design considerations of the facility are discussed and results are given to demonstrate its performance.

ISSN 0309-3069

National Physical Laboratory
Teddington, Middlesex, United Kingdom, TW11 OLW

Approved on behalf of Chief Executive, NPL
by Dr A R Colclough, Head
Division of Mechanical and Optical Metrology

CONTENTS

TABLES

FIGURE LEGENDS

1 INTRODUCTION

Multi-axis co-ordinate measuring machines (CMMs) are becoming an integral part of modern manufacturing industry. They are no longer restricted to the standards rooms but are now being used in production areas, forming part of a total quality system [1]. In the UK alone there are over 3000 CMMs measuring about £100M worth of manufactured parts *per annum*. Although it is of prime importance to the user to have an accurate estimate of the overall performance of a CMM, it is of key importance that the manufacturer knows how the individual elements of a CMM contribute to its overall performance [2]).

There are many sources of error associated with a CMM. It is now possible to obtain an error map of a CMM that can be used to correct partially for the geometrical systematic errors [3,4], examples of which are the straightness and squareness of the movement carriages. However, the measurement uncertainty introduced by the probe remains a significant proportion of the total measurement uncertainty of CMMs. In addition, a multi-axis probe system cannot be isolated easily from the rest of the measuring system. At present, probe calibration methods involving artefacts [5,6], whilst useful, are not always indicative of the probe performance as a completely independent functional unit.

The calibration facility described in this paper only calibrates contacting probes, *i.e.* those that mechanically contact the component being measured. There are two main types of contacting probe used on CMMs (although recently many more variations have become available [7]. First, there are 'touch trigger' probes that operate by generating a binary electronic pulse when the stylus ball contacts the component being measured. Secondly, there are analogue probes (also known as 'path-measuring' probes) which usually comprise three mutually-orthogonal spring flexures, the deflections of which are measured by three displacement transducers (normally inductive transformers). These probes measure the stylus ball position, relative to a fixed co-ordinate system within the body of the probe. In practice these co-ordinates are related to the linear scales of the measurement axes of the CMM to yield the co-ordinates of the measured point on a component. At NPL, high accuracy analogue probes are used in existing calibration services and it was an in-house requirement to develop a facility that could calibrate such probes. The calibration facility described in this paper does not calibrate touch trigger probes at present, although this is a future possibility.

The most accurate probes use a null-mode, static measurement technique in which the stylus ball contacts the component being measured causing a deflection of the stylus from its electrical zero position. The movement carriages of the CMM are then displaced until the probe indication returns to its electrical zero position where the co-ordinates of the machine carriages are recorded. This technique leads to three main sources of error, namely, zero point stability, reversal (hysteresis, previous position memory, *etc.*) and stylus and tip errors.

Zero point stability and reversal errors vary on the sensing mechanics and can be dependent on contact force, stylus geometry and the number of axes in which the probe can move. Suitable repeatability and scaling tests can quantify these errors. Errors caused by the geometry of the stylus and stem are proportional to the probing force and dependent on the material moduli, the stylus length and mean diameter. The friction between the workpiece and probe ball does not influence the measuring accuracy [8].

Errors will also arise in the flexure spring and transducer system. These will include: non-linearities in spring deformation characteristics, path-dependent systematic errors, mutual misalignment of the orthogonal flexure spring and transducer system, material inhomogeneities causing hysteresis and backlash, and calibration or gain errors inherent in the response characteristics of the transducers. The above sources of error have been the subject of a previous publication [9]. Errors may also be caused by the probe signal processing electronics. The combination of all the sources of error will normally lead to a measurement accuracy of between ± 0.5 to ± 1.0 μm throughout the entire work zone of a probe. The calibration facility described in this paper has a measurement uncertainty of ± 0.1 μm at a confidence level of 95%.

2 DESCRIPTION OF THE FACILITY

Figure 1 shows a photograph of the facility. The calibration facility employs a computer controlled three-axis flexure translation stage driven by stepping motors. The stage has a 2 mm range along each axis and a minimum step length of 0.1 μm. A block with a hemispherical recess in its top surface for mounting the probe and a system of three mutually-orthogonal plane mirrors are attached to the stage. The recess is made from Delrin (VT Plastics Ltd) and has the same radius as the probe's ball-ended stylus. The stylus ball sits in the recess and is constrained from above by a Delrin locking piece. This mounting system allows the probe stylus to rotate sufficiently freely about the z-axis so as to decrease the torsional forces on the probe. The recess and locking piece are easily manufactured for probes with different ball radii.

As the stage is moved the position of the centre of the ball stylus is measured in space by a 3-axis heterodyne interferometer system. Each of the three orthogonal mirrors forms part of a Hewlett-Packard 5501A double-pass laser-measurement system that measures the displacement of the stage in one axis. Figure 2 is a schema of the measurement system with the y-axis interferometer, normal to the plane of the paper, omitted for clarity. In operation, the stage is moved in steps and the co-ordinates from the probe and interferometers are compared; the axes measured by the interferometers act as the reference co-ordinate frame.

3 SYSTEM DESIGN

The facility has been designed to reduce the magnitude of its associated sources of uncertainty and to take advantage of comparative measurement techniques. Errors due to certain drifts or offsets are considered common to the separate components in the system. For example, mechanical sticking and slipping and the internal lubricants in the stage cause drifts which are common to the stage, the interferometer and the probe. However, errors arising due to drift in the probe signal conditioning electronics or due to non-linearities in its transducer system will be detected.

The lengths of the optical beam-paths that form part of the measurement loop of the interferometers have been minimised to avoid errors arising from fluctuations in the refractive index of the ambient air [10,11]. Over a period of one hour the peak-to-peak air temperature fluctuation is about 0.4 K. Values of air temperature, barometric pressure and humidity are measured at the start of a test and used, along with empirical equations [12,13], to calculate the refractive index of the air.

Thermal drift problems are compensated by the comparative nature of the measurement strategy and further reduced by operating the facility in a temperature-controlled environment. All critical parts of the facility are constructed of an alloy with a low coefficient of thermal expansion (Invar, Inco Alloys Ltd) and are kinematically mounted on a base-plate. Thermal expansion problems are further reduced by ensuring that the facility is thermally balanced, *i.e.* expansion in one part mechanically compensates expansion in another. These problems are most prominent in the z-axis of the probe calibration facility on account of the larger measurement loop required to accommodate the probe under test.

The largest error sources are the geometric effects due to Abbe offset [14] and are caused by angular guiding errors due to pitch and yaw in the motion of the 3-axis stage used. In the future, these errors could be reduced by using a stage with reduced geometrical errors. The three plane mirrors are mutually-orthogonal to within 5 seconds of arc and flat to less than $\lambda/20$ making them a negligible source of systematic measurement error.

4 MEASUREMENT PROCEDURES

In order that the characteristics of the probe may be assessed, three tests are carried out: repeatability, uni-axial response and volumetric accuracy.

4.1 REPEATABILITY

The repeatability is defined as the closeness of agreement of a group of measurements of the same measured quantity made by the same observer, using the same conditions, methods and apparatus. To evaluate the repeatability [15] the probe is moved from a start position to a point in its work zone, where the displacements measured by the interferometer and the probe are recorded, and back to the start position again. This measurement process is carried out a number of times for one, two or three axes and the repeatability is calculated.

4.2 UNI-AXIAL RESPONSE

The stage is moved in discrete increments in one axis through the work zone of the probe to measure its uni-axial response. The difference between the readings from the probe and interferometers are plotted against those from the interferometer and compared with the values obtained from a least-squares regression curve. From this data the RMS deviation of the probe's response from the regression curve can be calculated. Another significant parameter is the non-linearity of the probe defined by equation (4.1)

$$N = \frac{100N_{max}}{L} \% \qquad (4.1)$$

where N_{max} is the maximum deviation from the regression curve and L is the total displacement travelled in a test. It is important that tests are repeated a number of times, and an average obtained, to avoid outliers in the measurement data causing exaggerated values of non-linearity.

4.3 VOLUMETRIC ACCURACY

The stage is moved to a number of positions in the work zone of the probe and co-ordinate readings (relative to a datum) are taken. Figure 3 shows the path of the stage for a 27-point test. From the data the average errors in each co-ordinate can be calculated. In this paper the volumetric accuracy of a probe is defined as the average of the errors throughout the entire work zone given as an RMS value.

5 HARDWARE AND DATA ANALYSIS

All the measurement procedures and data acquisition are fully automated, using a PC, with the IEEE-488 interface bus and RS-232C serial interface. Analysis of the data is carried out by data processing algorithms available on NPL's mainframe computer using a fully tested and verified mathematical software package. From the data obtained using the tests described in section 4, various statistical parameters and graphical output can be obtained. Algorithms have been developed at NPL which mathematically rotate the co-ordinate frame of the probe transducer system into the co-ordinate system of the interferometers to minimise angular errors between the two co-ordinate frames. (The method used is to solve the three linear equations relating the two co-ordinate frames in a least squares sense using Given's method [16]. Any non-linearities in the response characteristics of the probe, scaling errors or mutual misalignment of the nominally orthogonal flexure spring and transducer system are not affected by the transformation. Once the data have been mathematically transformed and a rotation matrix obtained it is possible to calculate the out-of-squareness of the probe's flexure spring and transducer system. This systematic error will be a combination of the non-orthogonality of the probe's axes and the scaling errors.

Figure 4 shows a block diagram of the hardware in the facility. The probe's signal processing and conditioning electronics will be different depending on the probe manufacturer. The 3-axis probe used in this paper required a 24 bit parallel digital I/O interface card with a 37-way cable. The single axis probe used the IEEE-488 bus and a digital voltmeter.

6 UNCERTAINTIES

There are many sources of uncertainty associated with the laser interferometer measurement system. The various uncertainty terms have been described, in detail, in previous publications [17,18] and are summarised in the following sections. There are two different types of error: cumulative and non-cumulative. Cumulative error terms are expressed in parts-per-million (ppm) and are a function of the mean optical path length difference between the arms of the interferometer (the stage movement distance). Non-cumulative error terms are independent of measurement length.

6.1 CUMULATIVE ERROR TERMS

Wavelength stability

The source of the interferometer system is a calibrated frequency-stabilised He-Ne laser operating at a nominal wavelength of 633 nm. This value has a typical lifetime stability of ± 0.02 ppm. However, during a typical calibration test the stability is ± 0.002 ppm.

Atmospheric compensation

The laser wavelength is a function of the refractive index of the ambient atmosphere in which it operates. The refractive index is dependent upon the temperature, pressure, humidity and chemical composition of the ambient atmosphere. The software makes use of the modified equations due to Edlén to calculate a corrected value for the refractive index of the air using values of the ambient conditions measured immediately before a test. A 1 ppm length error corresponds to changes of 1 K in air temperature, 330 Pa in air pressure and 80% relative humidity.

At NPL the calibration facility resides in a room with temperature and humidity control. The peak-to-peak fluctuation in temperature over any 2 hour period is about 0.4 K. Only long volumetric accuracy tests would require this amount of time. The variation over the more normal measurement time of 15 minutes is about 0.1 K.

The atmospheric pressure will not be expected to change by more than about 40 Pa over 15 minutes, but in 2 hours it is possible for a weather front to pass over the laboratory causing a change in pressure of up to 800 Pa. Changes in the relative humidity and chemical composition will only be a few percent and can be considered negligible as regards this instrument.

Adding the two compensation error terms in quadrature (assuming they are randomly distributed) gives an uncertainty in length of ± 2.4 ppm over 2 hours and ± 0.11 ppm over 15 minutes. (Note that the rather high uncertainty term over two hours represents extreme pressure fluctuations.)

Cosine Error

There is always some misalignment of the measurement axis to the axis of motion of the

Optical non-linearity

Due to the inadvertent mixing of undesired polarisation components, caused by the imperfect optical coatings in the interferometer system, there is a non-linear relationship between the phase and displacement. This gives rise to a periodic error. In the case of the plane mirror interferometer the most extreme error is ± 2.4 nm. Other sources of optical non-linearity [19] give rise to negligible measurement uncertainties.

Optics Thermal Drift

As the temperature varies there is a change in the size of the optical components in the interferometer. In the case of the plane mirror interferometer with high stability adapter, the error is ± 0.01 ppm K^{-1}.

6.2.6 Abbe Error

The Abbe principle states that a measuring machine should always be designed so that the displacement measuring system is in line (co-axial) with the displacement to be measured. The error, ε, is given by equation (6.2)

$$\varepsilon = d \tan \alpha \qquad (6.2)$$

where d is the offset between the measurement axis and the centre of the stylus tip and α is the angular variation caused by the straightness of the plane mirror-stage system. In the case of a movement stage causing the displacement, any angular motion must be minimised. Using a double-pass plane mirror interferometer, the centre line between the incident and return beam is the measurement axis. The facility is designed in such a way as to minimise d which has been measured to be about 100 µm in extreme cases. The straightness errors due to the yaw and pitch of the stage can be measured by driving the stage, using an autocollimator and reflecting off the back faces of the plane mirrors. Where there are pitch and yaw errors, only the numerically greater value is used in the calculation of the Abbe error. There is no Abbe sensitivity to roll. The x-axis had the least angular error with a change of 20 seconds of arc over a 2 mm travel length. The y-axis had a change of 55 seconds of arc and the z-axis had a change of 85 seconds of arc. These correspond to Abbe errors of roughly ± 10, ± 30 and ± 40 nm for the x, y and z axes respectively. The double pass interferometer system compensates for Abbe error when measuring in one axis only.

Random Errors

The overall uncertainty due to random effects such as acoustic noise, vibration and air turbulence, was determined by repeatedly reading the displacement values measured by the interferometers. A standard deviation of ± 10 nm was calculated from 50 such static measurements. Note that this term will also contain components of the other terms stated above.

6.3 OVERALL UNCERTAINTY IN MEASUREMENT

The results of the analysis of the various systematic and random uncertainties associated with the facility are shown in Table 1. Assuming all the errors are normally-distributed, the final statement should be multiplied by a coverage factor of 1.96 to give a 95% level of confidence [20]. It is well to note that the assumption of normality is not correct for some errors, such as those due to the resolution of the interferometer and the Abbe offset. If, however, it is assumed that these errors have a rectangular distribution, the uncertainty, with 95% confidence, is given by the coverage factor multiplied by the standard deviation [21,22], where the standard deviation is the semi-range divided by $\sqrt{3}$.

that the single-axis response of the probe is dominated by random noise and is not position dependent .

7.3 VOLUMETRIC ACCURACY

A number of one thousand-point tests were carried out throughout the entire work zone of the probe and the volumetric accuracy values were calculated to be 230, 140 and 95 nm for the x-, y- and z-axes respectively. Figure 9 shows the y-axis errors of the probe in one xy-plane. Once again the dominant error term is caused by random noise.

7.4 MUTUAL ANGLES

The mutual angles between the axes of the probe's flexure spring and transducer system were calculated to be 90.3°, 87.2° and 91.6° for the xy-, yz- and xz-angles respectively. In the case of the angle between the y- and z-axes this corresponds to an error in position of 240 nm over the full 200 µm work zone of the probe. This is clearly an important component of the probe's systematic errors.

7.5 REPEATABILITY WITH THE NSMMM

In order to show that constraining the probe does not affect its measurement performance, repeatability tests were also carried out on the NSMMM at NPL by having the movement carriages repeatedly move a gauge block in and out of contact with the probe. The NSMMM is expected to have a uni-axial repeatability, over the back-off distances employed (between 10 and 80 µm), of the same order of magnitude as the high-accuracy probe under test. (A slightly less accurate result may be expected because the mounting system on the NSMMM is subject to greater thermal and vibration effects.). Under these conditions the repeatability values of the probe were ± 320, ± 250 and ± 350 nm for the x-, y- and z-axes respectively. These results compare favourably with those obtained with the probe calibration facility to within the accuracy expected of the NSMMM. This indicates that the mounting system employed by the calibration facility does not over-constrain the movement of the probe and realistically represents a probe in its working, CMM, environment.

7.6 CALIBRATION OF AN LVDT PROBE

To test further the performance of the facility the Delrin recess was replaced by a gauge block and a very high-accuracy single axis, LVDT, lever-type probe was repeatedly contacted by moving the 3-axis stage in one axis only. Figure 10 shows the results of an 80 µm back-off distance repeatability test. The linear drift component is common to both the probe and the calibration facility and is, effectively, filtered out of the repeatability data by taking the difference between the displacements measured by the interferometers and the LVDT probe. The probe was found to have a repeatability [15] of ± 70 nm and a non-linearity of 3% over its linear measuring range (± 0.3 mm). These values are less than those quoted by the manufacturer of the probe.

8 CONCLUSION

The facility described in this paper serves the purpose of calibrating analogue probes to within an accuracy required by users and manufacturers of high-accuracy probes and CMMs. The repeatability of a high accuracy analogue probe has been measured and found to be independent of back-off distance. Results of repeatability tests carried out with the probe mounted on the NSMMM agree with those obtained using the calibration facility. The linear response and volumetric accuracy tests provide the user of the probe with an overall accuracy statement and the test data can be used as a basis for probe error compensation by the CMM's software [24]. The z-axis was found to be more accurate than the x- and y-axes.

stage. In this facility the measurement axis is the beam-path of the laser. This misalignment manifests itself as an error in the measured length which is directly proportional to the cosine of the angle between the measurement and motion axes. The cosine error always causes the interferometer to measure shorter than the actual distance travelled by the stage. With the interferometer block removed, the cosine error can be found by auto-reflecting the laser beam and estimating the misalignment as the stage is moved through its full range. If the beam were perfectly aligned the reflected beam would be superimposed on the laser aperture. The worst case measured was a displacement from the aperture of 2 mm for a path-length of about 1 m. This corresponds to a cosine error of 2 ppm. Over a 200 μm range the uncertainty in measured length due to this error would be negligible.

Deadpath Error

An error will arise due to the uncompensated path of the laser beam between the interferometer block and the plane mirror at the zero position of the stage. This is the deadpath error arising from the fact that the reference and measurement components of the beam are different. Deadpath error is not a function of the measurement length but of the length of the deadpath. It is therefore a systematic error which is constant for a given system set up. Considering this error term the displacement measured, D, is given by equation (6.1)

$$D \qquad \frac{N\lambda_{vac}}{} - \frac{\Delta n d}{} \qquad (6.1)$$

where d is the deadpath length, N is half the number of fringes counted during the displacement, λ_{vac} is the wavelength of the laser in vacuo, n_2 is the refractive index at the end of the measurement, Δn the change in refractive index over the measurement time: that is $n_2 = n_1 + \Delta n$, and n_1 is the refractive index at the start of the test. The second term on the right hand side of equation (6.1) is the deadpath error. Considering the changes in atmospheric conditions discussed in section 6.1.2 and a deadpath length of 15 mm the magnitude of the deadpath error over a 2 hour period is ± 30 nm.

6.2 NON-CUMULATIVE ERROR TERMS

Error in the Edlén Equation

The modified equation due to Edlén that is used to calculate the correction for the wavelength of the laser in ambient air has an uncertainty of ± 10 nm.

System Thermal Expansion Error

Due to the variations in air temperature there will be an error caused by the thermal expansion of the materials in the facility. Most of the critical parts of the facility are constructed from low expansion materials to reduce this problem. The uncertainty component due to thermal expansion has been calculated to be ± 10 nm by considering the dimensions of the facility and values of the coefficients of thermal expansion.

Electronics Error

The resolution of the laser interferometer is limited by non-linearity and noise in the fringe counting electronics. The principle noise source is the quantisation noise due to the analogue to digital converter. In a plane mirror system the resolution is ± 5 nm.

The repeatability is defined quantitatively in BS5532 : Part 1 (1978 *Statistical terminology* British Standards Institution) as the sample standard deviation of the measured results multiplied by a factor which represents the level of statistical confidence. In the case of the 3-axis probe the distributions observed were found to be rectangular and the standard deviation has been defined as the semi-range of the results divided by √3. The confidence level used is 95%.

Searle S R 1982 *Matrix Algebra useful for Statistics* (John Wiley & Sons: USA)

Steinmetz C, Burgoon R, Herris J 1987 Accuracy analysis and improvements to the Hewlett-Packard laser interferometer system *Proc. SPIE Interferometric Metrology* **816** 79-94

Achieving maximum accuracy and repeatability with the HP 5527A laser position transducer system Product note 5527A-2 (Hewlett Packard)

Rosenbluth A E, Bobroff N 1990 Optical sources of non-linearity in heterodyne interferometers *Precision Engineering* **12** (1) 7-11

Campion P J, Burns J E, Williams A 1980 *A code of practice for the detailed statement of accuracy* (NPL: Crown copyright)

Neyman J, Pearson E S 1928 On the use and interpretation of certain test criteria for purposes of statistical inference Part 1 *Biometrika* **20A** 175-240

Dietrich C F 1991 *Uncertainty, calibration and probability* 2nd Edn. (Adam Hilger: Bristol, Philadelphia and New York)

The NSMMM is a modified Moore M-48Z measuring machine with a laser interferometric tracking system and extensive software error correction

Shin Y C, Wei Y 1992 A statistical analysis of positional errors of a multiaxis machine tool *Precision Engineering* **14**(3) 139-146

Where the uncertainty values for one axis may be higher in magnitude than for the other axes (as is the case with the thermal expansion and Abbe terms) the higher term has been used to calculate the overall uncertainty. The final uncertainty is calculated by adding the various terms in quadrature and multiplying by 1.96. The uncertainties in Table 1 have been calculated for a measurement time of 2 hours, although repeatability and uni-axis tests only take about 15 minutes. The overall uncertainty would be expected to be smaller for relatively fast tests. As an example, the measurement uncertainty for a single axis LVDT plunger-type probe, with a measurement time of 15 minutes and using a single axis, would be about ± 0.04 μm at a confidence level of 95%.

7 RESULTS

Tests were carried out using a high-accuracy, 3-axis analogue probe. This had a maximum linear measuring range in each axis of ± 0.1 mm and a nominal resolution of 25 nm. A 60 mm long, ball-ended, ruby stylus of radius 2 mm and probing force 0.05 N was used. Repeatability tests were also carried out using the National Standard Multi-axis Measuring Machine [23] (NSMMM) and a single-axis lever-type LVDT probe.

7.1 REPEATABILITY

Single-axis repeatability tests were carried out by taking 50 repeated measurements of moving from a reference point and returning to it. (The distance moved from the reference point is known as the 'back-off' distance). This was repeated for each axis in opposite directions of approach and over two back-off distances - 10 and 80 μm. The repeatability values, calculated by taking the mean of the results obtained in both directions of approach, are shown in Table 2. Figures 5 and 6 show typical histograms of the x-axis repeatability data for 10 μm and 80 μm back-off distances. The results for all three axes are very similar, although the z-axis is consistently more accurate, probably because probing in the z direction is more symmetrical and not as susceptible to errors caused by distortion of the stylus and stem.

The histograms observed have essentially rectangular distributions. The non-normality of the distributions indicates that there are very few sources of random error contributing to the overall random uncertainty (Central Limit theorem). No hysteresis was observed in any axis as the direction of approach was reversed and there is no significant difference between the results obtained over the two back-off distances. This is a useful, and unexpected, result suggesting that the repeatability of the probe is the same throughout its entire work zone.

During the repeatability tests a consistent linear drift component was observed if the probe was not given at least 5 hours to stabilise once switched on. This would tend to increase the spread in the readings and skew the distributions. Figure 7 shows the results of a 12 hour repeatability test and clearly shows the time required for the probe to stabilise. The drift in the probe readings was not found to correlate with measured air temperature or atmospheric pressure variations and would appear to represent mechanical or electrical transients caused by self-heating and stress release within the probe and its corresponding signal conditioning electronics.

7.2 UNI-AXIAL RESPONSE

The stage was moved through the work zone of the probe five times in each axis and for each direction of approach (ten tests per axis). Figure 8 shows the stage position along the x-axis against residual probe readings, *i.e.* the stage position as measured by the interferometers minus that measured by the probe. The RMS deviations from the regression curve were 143, 144 and 94 nm for the x-, y- and z-axes respectively. The plots show random fluctuations and there is no cross-correlation between one plot and another. The calculated values of non-linearity were found to be less than 0.5%, for all three axes, which indicates

TABLES

Table 1 Uncertainty terms for the NPL probe calibration facility. The measurement length, L, is in millimetres.

Type of error	**Uncertainty/nm**
Wavelength stability	$\pm 0.02\,L$
Atmospheric compensation	$\pm 2.4\,L$
Cosine error	$\pm 2\,L$
Edlén equation	± 10
Deadpath length	± 30
Thermal expansion	± 10
Electronics	± 5
Optics non-linearity	± 2.4
Optics thermal drift	± 2
Abbe offset	± 40
Random errors	± 10
Total uncertainty	$\pm \sqrt{[(50)^2 + (3L)^2]}$

Table 2 Repeatability results

		Repeatability	**/ nm**
Back-off / µm	x-axis	y-axis	z-axis
10	± 270	± 230	± 185
80	± 270	± 230	± 200

FIGURE LEGENDS

Figure 1	The calibration facility
Figure 2	Schema of the calibration facility
Figure 3	Path of the stage during a 27-point volumetric accuracy test
Figure 4	Block diagram of the hardware
Figure 5	Histogram depicting repeatability results for the x-axis of the probe over a back-off distance of 10 μm and for 50 measurements
Figure 6	Histogram depicting repeatability results for the x-axis of the probe over a back-off distance of 80 μm and for 50 measurements
Figure 7	Drift test results over a 12 hour period
Figure 8	X-axis uni-axial response results
Figure 9	Errors in y-axis for one xy-plane
Figure 10	Uni-axis probe repeatability results

The squareness values obtained from the volumetric accuracy test would prove very useful to the user of a probe as they would be easy to correct using the machine software. At present the facility is available to industry and academia, as an NPL measurement service, for calibrating single- and multi-axis analogue probes.

ACKNOWLEDGEMENTS

The author would like to thank Dr G N Peggs, N R Cross, D R Flack and P Nath for help and discussions. He would also like to acknowledge the work carried out by NPL Engineering Services on design and construction of the facility and by G T Anthony for mathematical algorithms.

9 REFERENCES

[1] Jones B E 1987 Sensors in industrial metrology *J. Phys. E: Sci. Instrum.* **20** 1113-1126

[2] Peggs G N 1989 Creating a standards infrastructure for co-ordinate measurement technology in the *UK Ann. CIRP* **38** 521-522

[3] Soons J A, Theuws F C, Scellekens P H 1992 Modelling the errors of multi-axis machines: a general methodology *Precision Engineering* **14**(1) 5-19

[4] Burdekin M, Giacoma B D, Xijing Z 1985 Calibration software and applications to co-ordinate measuring machines *Proceedings of NPL conference 'Software for co-ordinate measuring machines'*, 1-8

[5] Butler C 1991 An investigation into the performance of probes on coordinate measuring machines *Industrial Metrology* **2** 59-70

[6] Peggs G N 1991 A review of the methods for the accurate metrology of complex three-dimensional components and artefacts *NPL Report* **MOM 101**

[7] Butler C, Gregoriou G, Shams 1989 Sensors in automatic inspection *Proceedings of Mechatronics '89*

[8] Lotze W 1994 Multidimensional measuring probe head improves accuracy and functionality of coordinate measuring machines *Measurement* **13** 91-97

[9] Pfeifer T, Bambach M, Fürst A 1979 Determination of the measuring error of 3-D sensing systems *Technisches Messen* **2** 47-52 and **4** 161-169

Zanoni C A 1988 High precision interferometric linear and angular displacement metrology *Zygo Corporation Document*

Downs M J 1989 Achievement of the optimum performance from laser interferometer systems when applied to precision length measurement in the free atmosphere *NPL Report* **MOM 92**

Edlén B 1966 The refractive index of air *Metrologia* **2**(2) 71-80

Birch K P, Downs M J 1988 The results of a comparison between calculated and measured values of the refractive index of air *J. Phys. E: Sci. Instrum.* **21** 694-695

Bryan J B 1979 The Abbe principle revisited: an updated interpretation *Precision Engineering* **1** 129-132

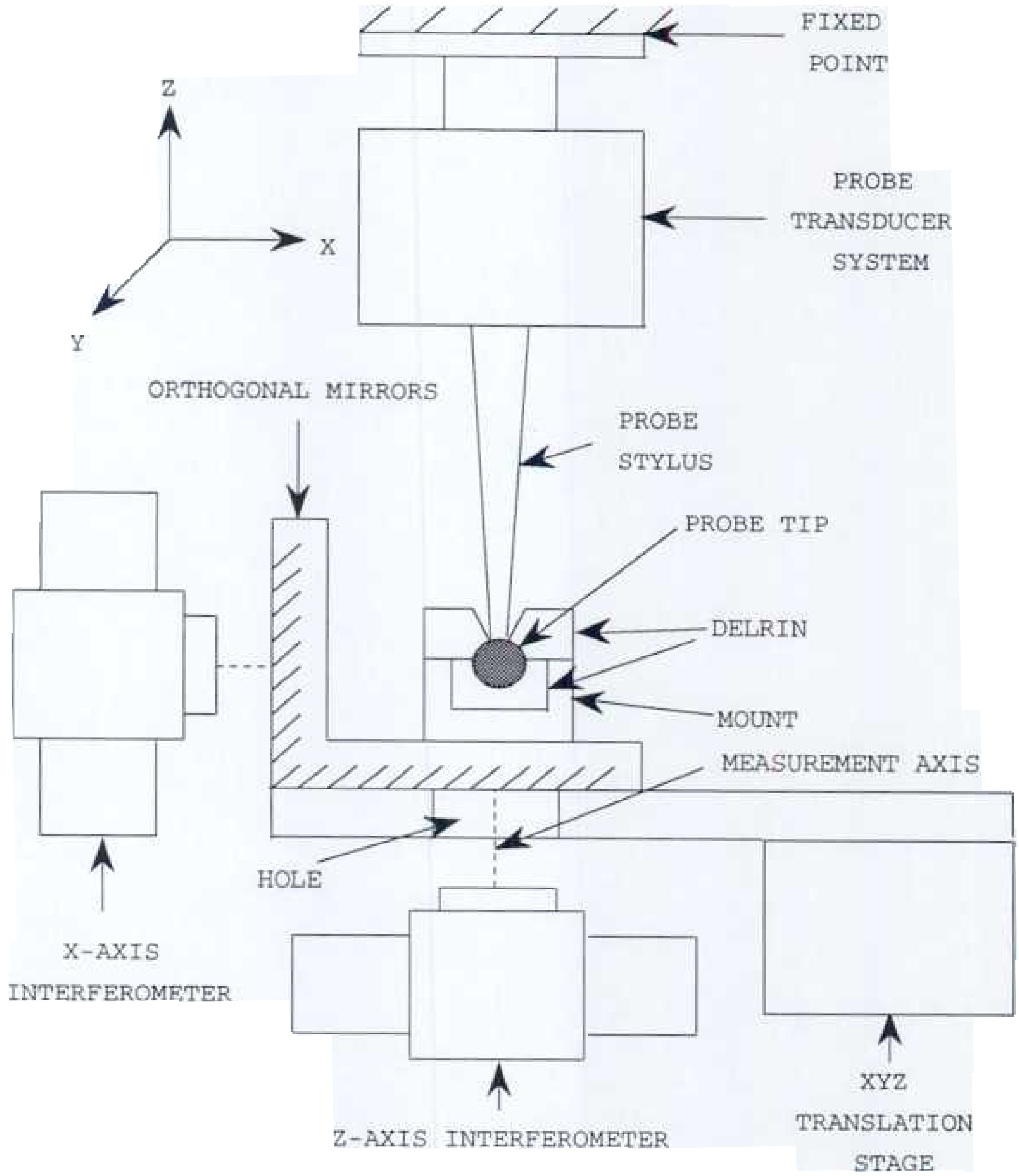
FIXED
POINT
Z
X
Y
PROBE
TRANSDUCER
SYSTEM
ORTHOGONAL MIRRORS
PROBE
STYLUS
PROBE TIP
DELRIN
MOUNT
MEASUREMENT AXIS
HOLE
X-AXIS
INTERFEROMETER
Z-AXIS INTERFEROMETER
XYZ
TRANSLATION
STAGE

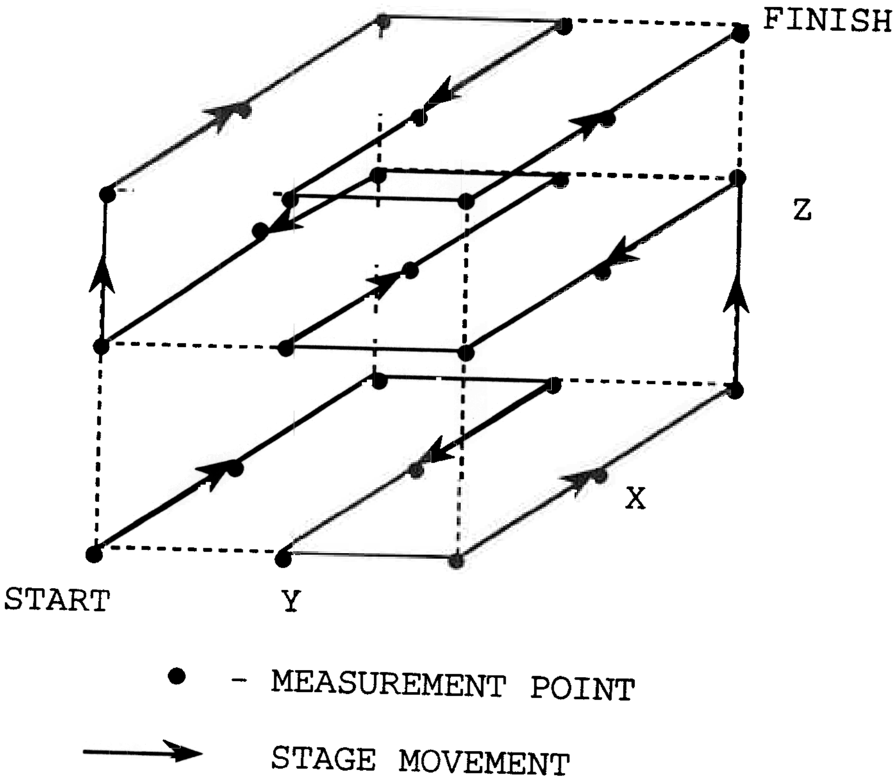
FINISH
Z
X
START
Y
- MEASUREMENT POINT
STAGE MOVEMENT

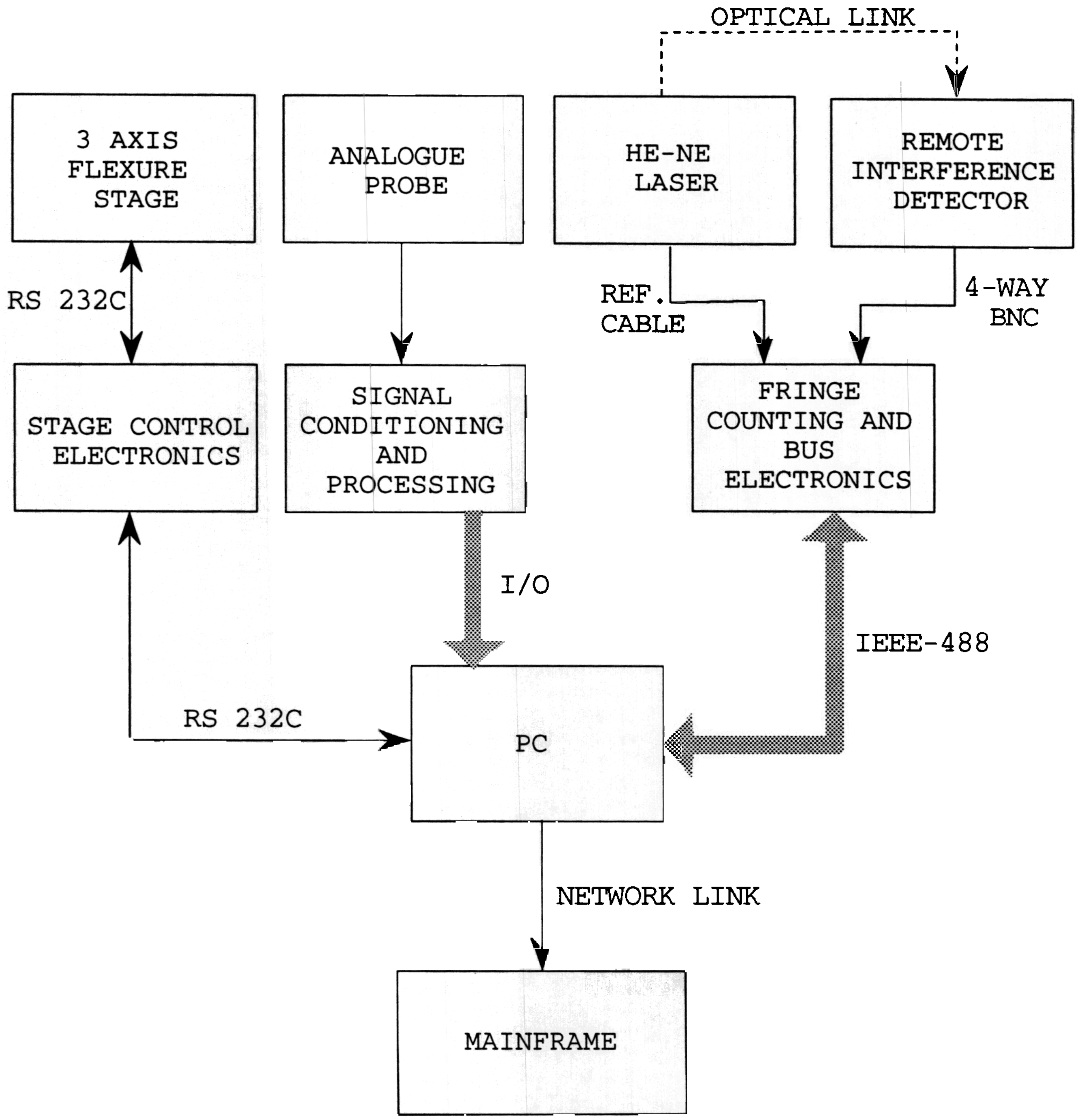
OPTICAL LINK
3 AXIS FLEXURE STAGE
ANALOGUE PROBE
HE-NE LASER
REMOTE INTERFERENCE DETECTOR
RS 232C
REF. CABLE
4-WAY BNC
STAGE CONTROL ELECTRONICS
SIGNAL CONDITIONING AND PROCESSING
FRINGE COUNTING AND BUS ELECTRONICS
I/O
IEEE-488
RS 232C
PC
NETWORK LINK
MAINFRAME

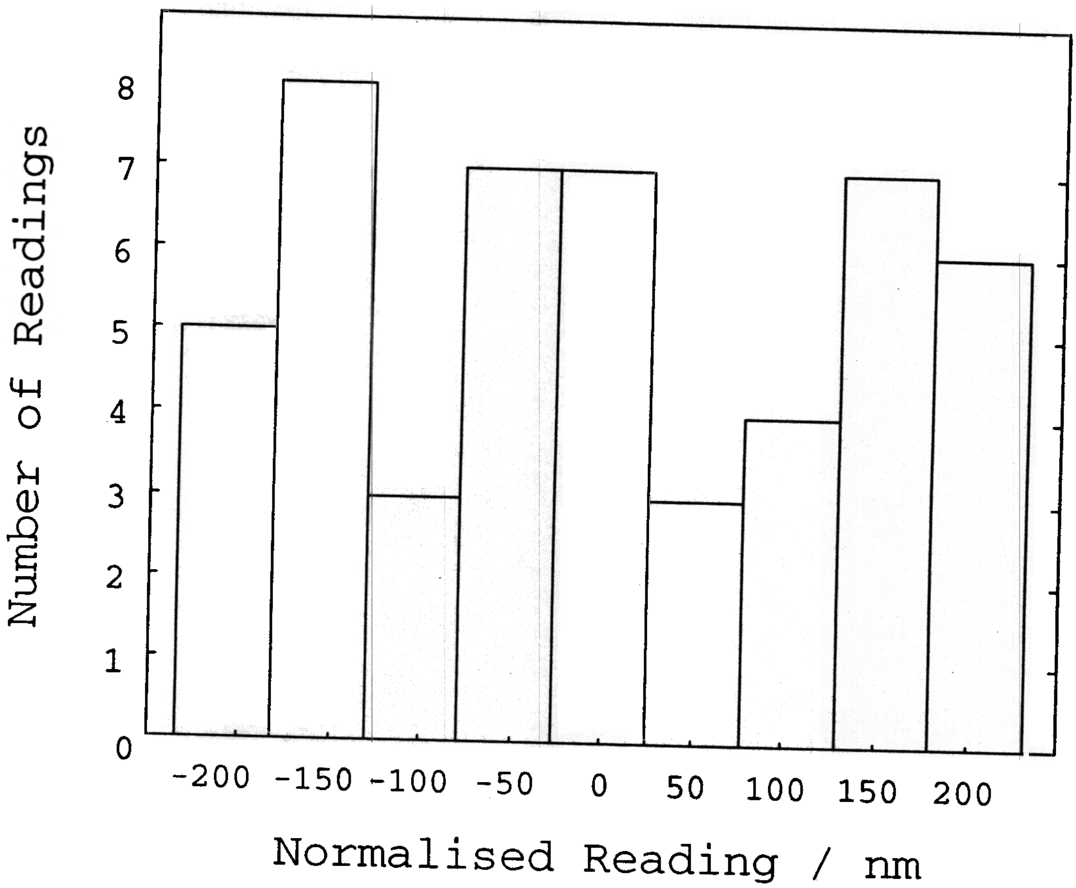
Number of Readings
8
7
6
5
4
3
2
1
0
-200
-150
-100
-50
0
50
100
150
200
Normalised Reading / nm

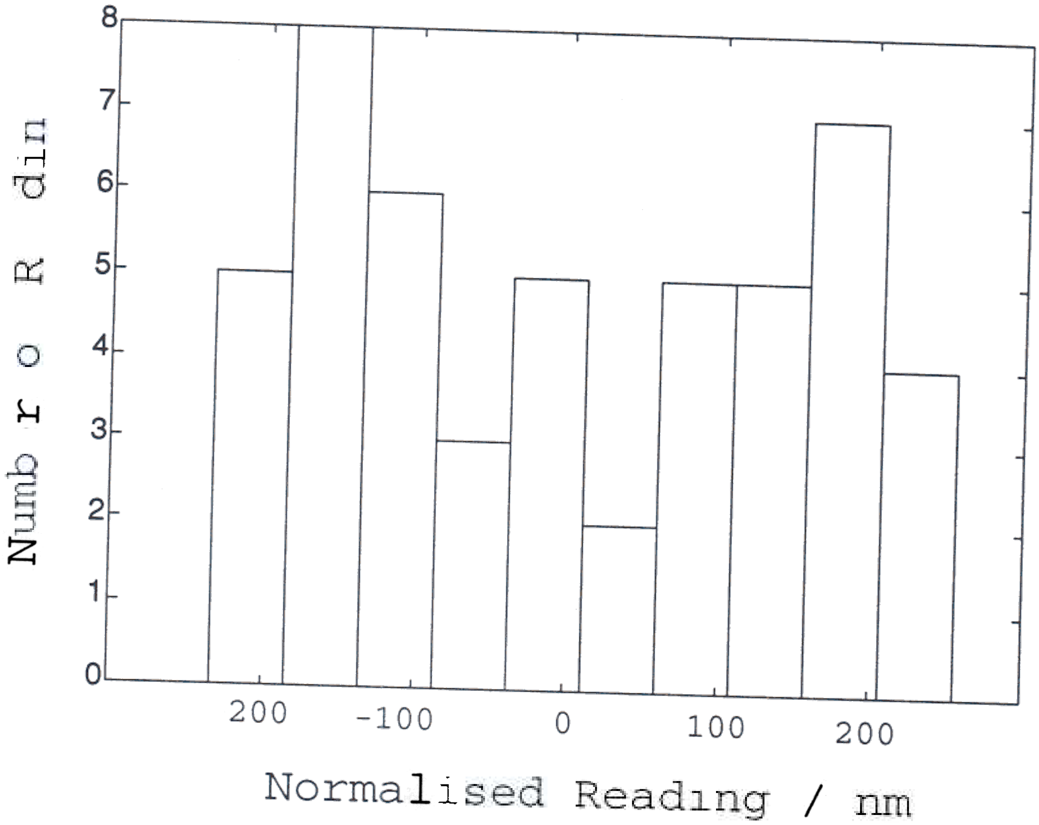
Numb r o R din
0
1
2
3
4
5
6
7
8
200
-100
0
100
200
Normalised Reading / nm

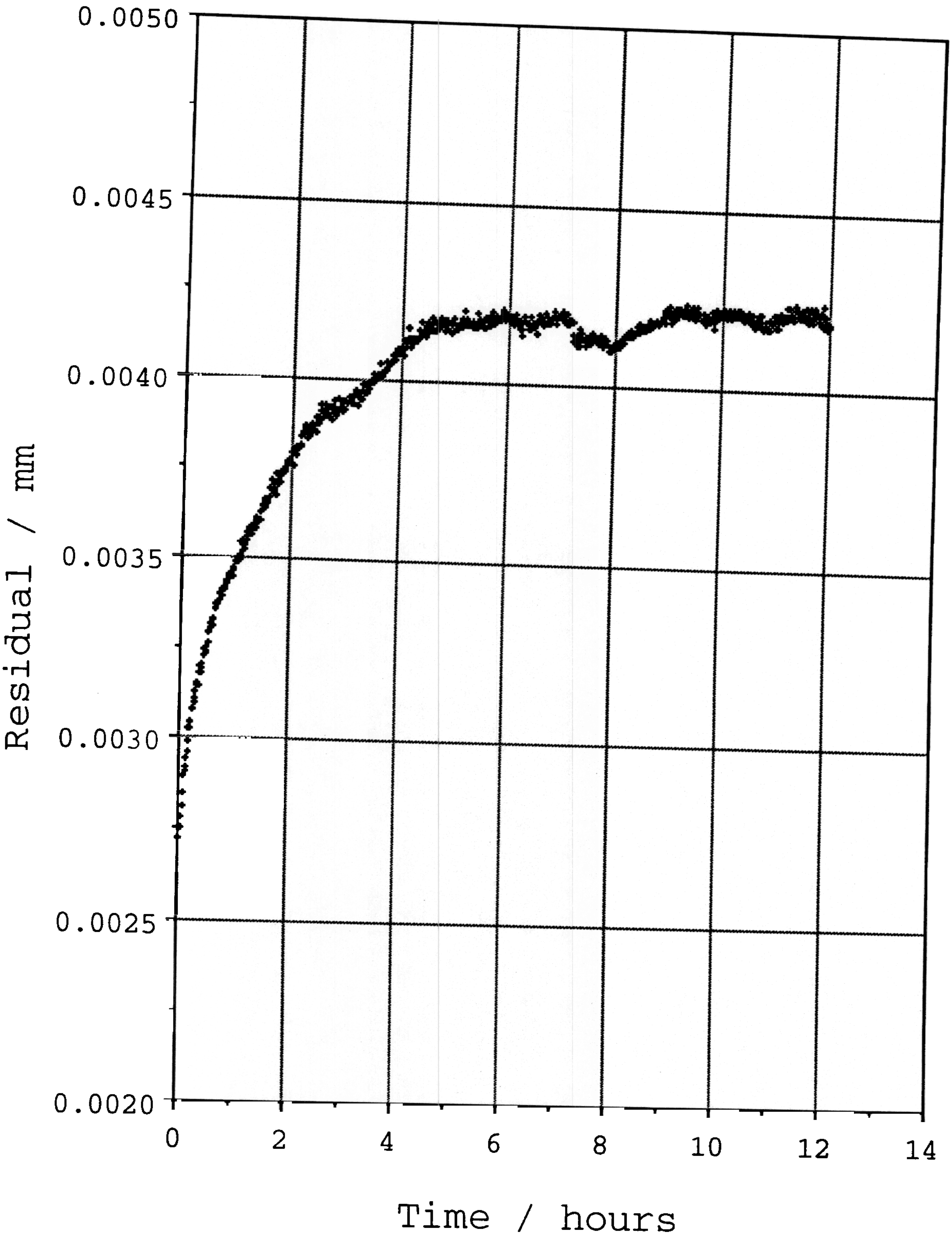
0.0050
0.0045
0.0040
0.0035
0.0030
0.0025
0.0020
Residual / mm
0
2
4
6
8
10
12
14
Time / hours

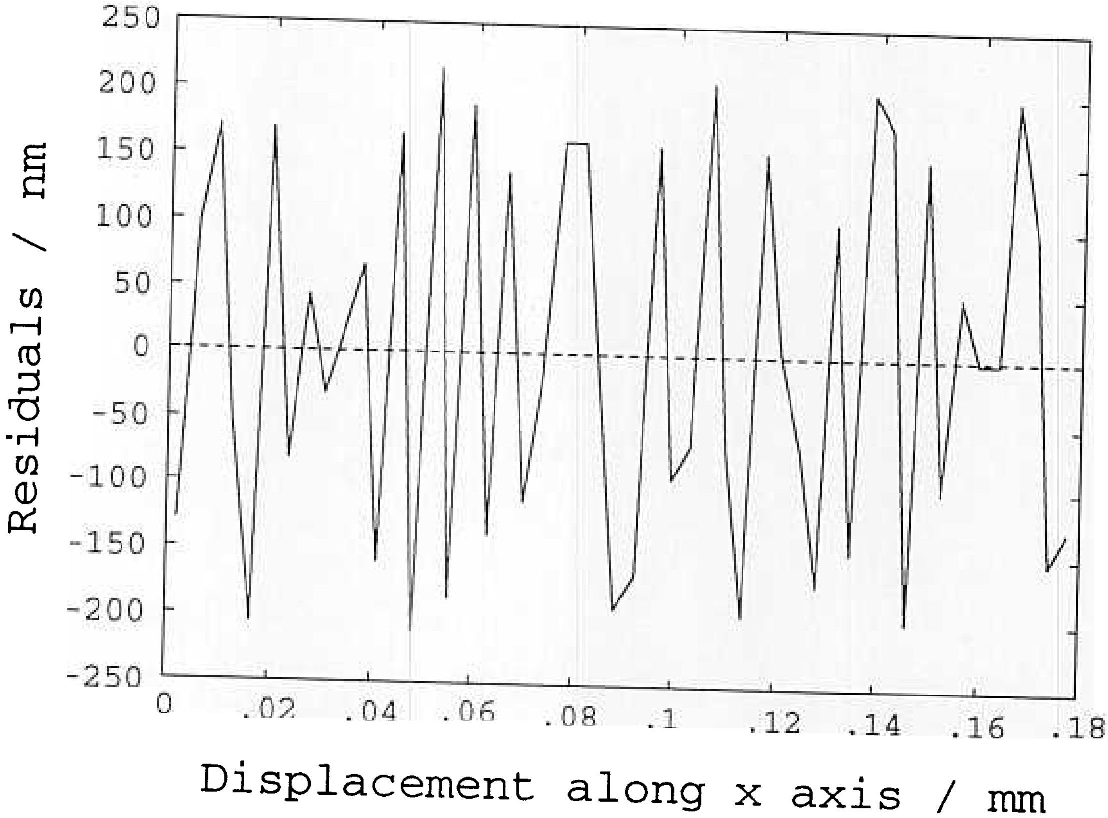

250
200
150
100
50
0
-50
-100
-150
-200
-250
Residuals / nm
0
.02
.04
.06
.08
.1
.12
.14
.16
.18
Displacement along x axis / mm

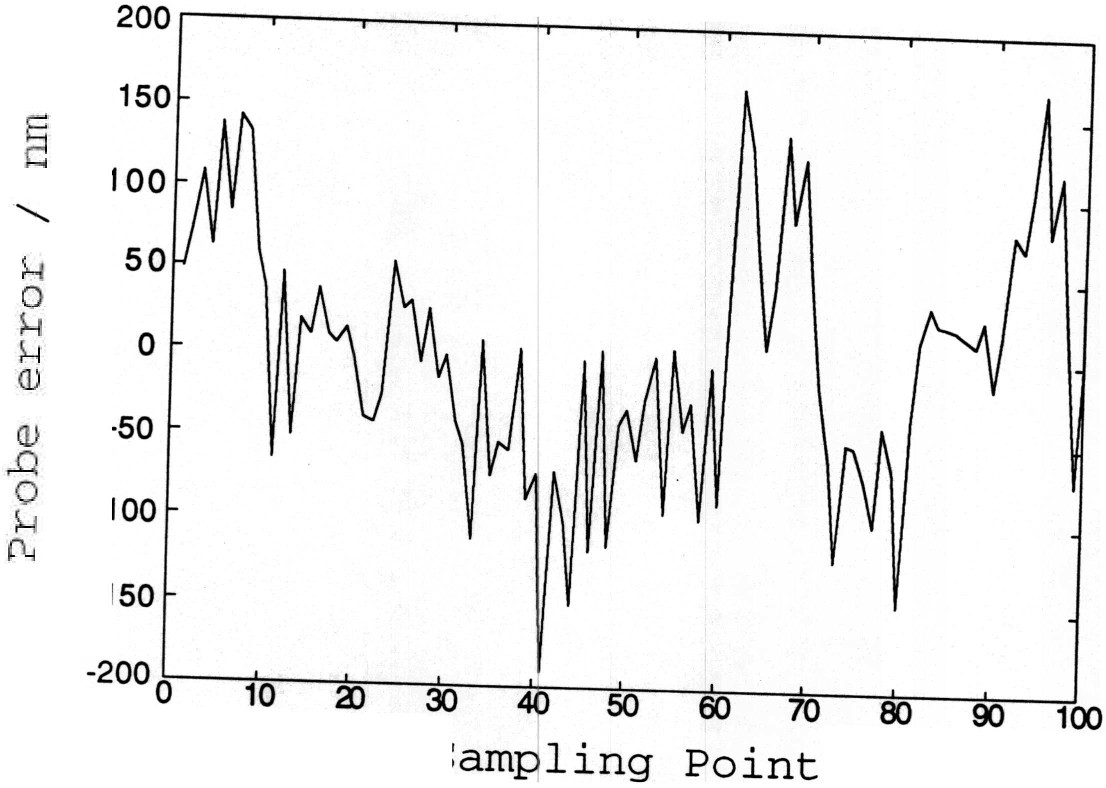

Probe error / nm
200
150
100
50
0
-50
100
150
-200
0
10
20
30
40
50
60
70
80
90
100
ampling Point

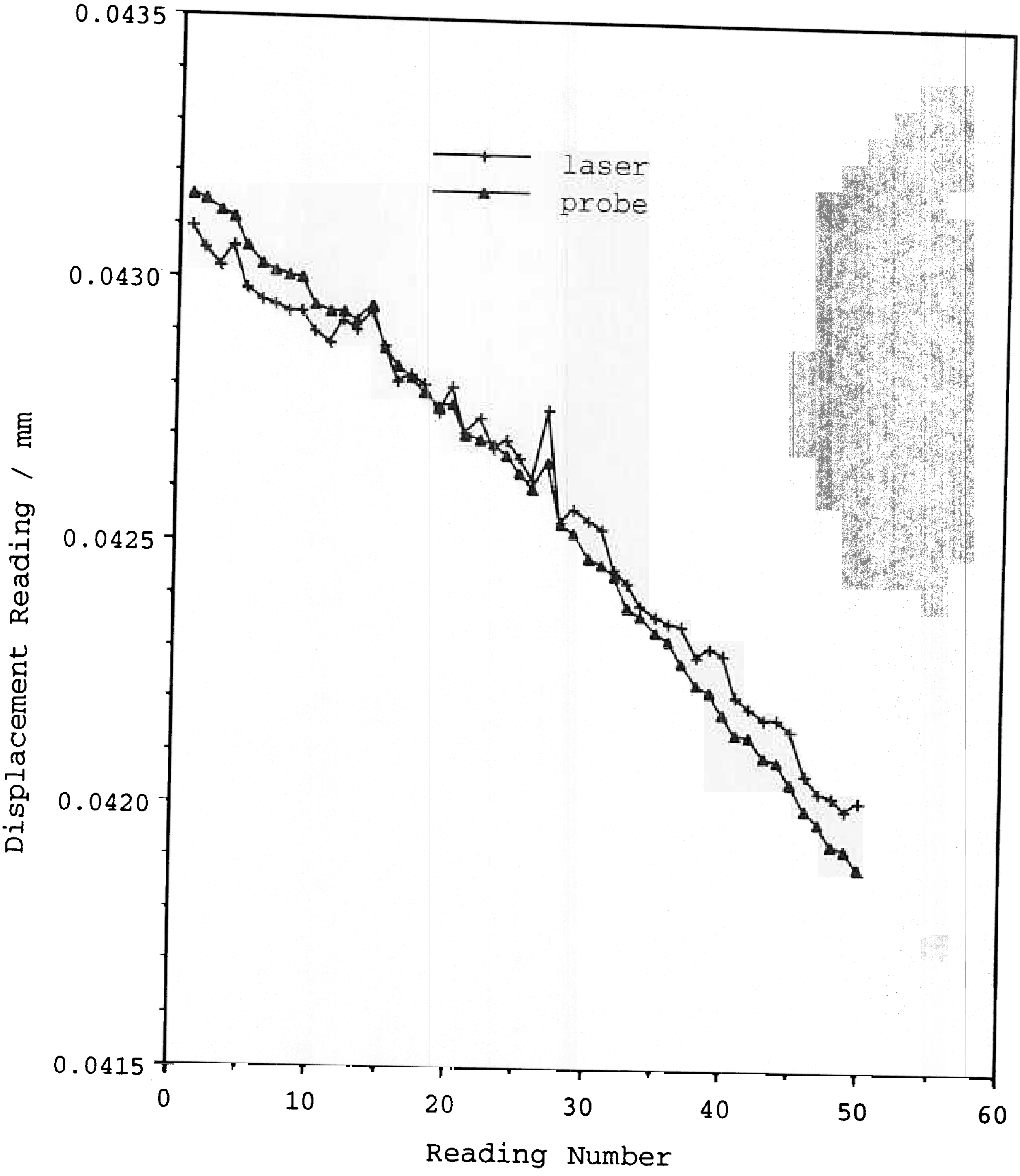

0.0435
0.0430
0.0425
0.0420
0.0415
Displacement Reading / mm
laser
probe
0
10
20
30
40
50
60
Reading Number